Journal of Applied Polymer Science

In Situ Preparation of Resol/Clay Nanocomposites

Nilgün Kızılcan, Gözde Özkaraman

Department of Chemistry, Faculty of Science, Istanbul Technical University, 34469-Maslak, Istanbul, Turkey
Correspondence to: N. Kızılcan (E-mail: kizilcan@itu.edu.tr) or G. Özkaraman
(E-mail: gozkaraman@itu.edu.tr or morr.go@hotmail.com)

ABSTRACT: In this study, *in situ* modified phenol formaldehyde resins were prepared from hydroxyl terminated polydimethyl siloxane (DH.PDMS), clay (montmorillonite) in the presence of base catalyst. Different clay contents (0.5, 1, 3, 5 wt %) were used to produce DH.PDMS modified resol/clay nanocomposite resins (DH.PDMS-LC-PFRs). DH.PDMS-LC-PFRs were partially cured by heat, and the effects of the curing process and the clay content in the resol resin were determined on the spectroscopic, thermal, mechanical and microscopic properties of the final products. Furthermore, the effects of the reaction time on the polymerization and on the morphology of the materials were investigated. The structures of the specimens were characterized by means of Fourier Transform Infrared (FTIR-ATR) spectroscopy. Thermal properties of the samples were determined with Differential Scanning Calorimeter (DSC) and Thermogravimetric Analyzer (TGA). Mechanical properties of the specimens were determined by Dynamic Mechanical Analyzer (DMA). The obtained samples were also characterized morphologically by Scanning Electron Microscope (SEM). © 2013 Wiley Periodicals, Inc. J. Appl. Polym. Sci. 129: 2966–2976, 2013

KEYWORDS: clay; resins; polycondensation; thermosets; composites

Received 4 June 2012; accepted 10 January 2013; published online 15 February 2013
DOI: 10.1002/app.39013

INTRODUCTION

Commercial resins are generally solid materials with low molecular weight and they can be processed easily. Resins are mainly used in surface coatings, varnishes, inks, and textile and paper industries. Previous studies demonstrated the synthesis of copolymers of ketonic resins is possible with diamine terminated polydimethylsiloxanes and DH.PDMS by one step method of in situ modification of ketonic resin.[1] Polysiloxanes have many interesting properties such as their high surface activities and low solubility parameters. These properties result in the thermodynamic incompatibility of polysiloxanes with most other organic polymer systems. Siloxane-containing copolymers are used as compatibilizers along with organic polymers in order to overcome these difficulties. Siloxane segments of the copolymers migrate to the air–polymer surface in siloxane-containing copolymers, but the organic segments act as an anchoring group for the siloxane blocks, so that permanent surface modification can be obtained for resins.

Nanocomposites produced by organic polymers and inorganic clay minerals containing silicate layers such as montmorillonite (MMT) have attracted great interest due to adventitious improvements in mechanical, thermal, barrier and clarity properties without a significant increase in density, which is not possible with conventional fillers.[2–9] Layered silicates used commonly in preparation of polymer layered silicate nanocomposites belong to general family of 2 : 1 phyllosilicates. Montmorillonite, hectorite, and saponite are the most commonly used layered silicates. To render layered silicates miscible with the polymer matrices, hydrophilic silicate surface should be converted to an organophilic surface, this process makes the intercalation of many engineering polymers possible.[10] Polymer/layered silicate (P/LS) nanocomposites generally improve properties of polymeric materials, even at very low volume fraction loading (1–5%) of layered silicates; opposed to the high volume fraction loading (⟫50%) in the traditional advanced composites.[11] Nanometer size particles in a (polymer/ceramic/metal) matrix disperse in order to form nanocomposites. The polymers containing layered silicate clay minerals as reinforcing agent can be classified as speared (intercalated) or dispersed (exfoliated) depending on dispersion of clay in the matrix.[12–14] Hybrid organic–inorganic substances composed of nanometer-sized particles are dispersed in a polymer matrix known as polymer/clay nanocomposites. Clays exhibit plastic behavior upon heat, and they remain as hard materials at elevated temperatures. The distribution of inorganic materials in the polymer matrix is a very

© 2013 Wiley Periodicals, Inc.

important issue in the preparation of nanocomposites. Improper achievement of exfoliation causes clusters of inorganic materials in the polymer matrix and this limits the improvement of the properties.[15]

Polymeric composites and recently nanocomposites have received widespread attention due to the dramatic improvements in the performance of polymers through the incorporation of micro and nanosized fillers. Some of the important classes of nanoparticles used as fillers in polymeric composites include furned silica, organoclays, carbon nanofibers, carbon nanotubes, titanium oxide and very recently graphene. Many polymers have been used as hosts for the preparation of composites based on such fillers. Such composites have in general displayed highly improved thermal, mechanical and engineering properties when compared with their virgin resins.[16]

Phenolic resins were the first thermosetting resins to be synthesized in 1907.[17] Phenolic resins have been widely used due to their utterly ablative properties, structural integrities, thermal stabilities, and solvent resistances that make them advantageous as thermal insulation materials, in wood products industry, coatings, molding compounds, foundry, and composite materials.[18–22] Manfredi et al.[23] have been characterized several resol in solution with variable formaldehyde to phenol (F/Ph) molar ratios before the crosslinking reaction. The addition of layered silicates to the phenolic resins could increase their thermal resistance and mechanical properties. For thermoset polymers, a significant amount of research has been performed on nanocomposites with epoxy resins.[24] However, phenolic resin/clay nanocomposites have not been studied on as much as epoxy resins due to the three-dimensional (3D) network structure of the phenolics, that is present even before crosslinking. This network structure is the result of polyfunctionality of phenol having more than one reactive site for aromatic substitution reaction and excess of formaldehyde. Their structure makes it more difficult than linear polymer for intercalating layered silicate galleries. Byun et al.[25] performed the first study about forming nanocomposites from resole type phenolic resin layered silicate nanocomposites using various layered silicates by melt intercalation. They have concluded that exfoliation was more difficult with resol type phenolic resins than novolac type phenolic resins due to the 3D structure of the resol resins even before curing. These structural peculiarities may cause resins to be too bulky to synthesize a nanocomposite, especially compared to other thermosetting resins such as widely studied epoxy or even novolac type phenolic resins, which are rather linear and easier to intercalate.[26] Manfredi et al.[27] studied the influence of nanoreinforcement in the curing process and in the final properties of the cured resin. Kaynak and Tasan investigated the effects of several production parameters on the structure of resol type phenolic resin/layered silicate nanocomposites.[28] Lopez et al.[29] performed studies on curing characteristics of resol/layered silicate nanocomposites and they investigated the effects of clay content in a resol resin on curing process by DSC and FTIR.

In this study, nanocomposites of resol resins were synthesized by direct addition of different contents (from 0.5 to 5 wt %) of clay into synthesis media. During synthesis DH.PDMS have also been added in the media to improve the surface properties of the material. With this method DH.PDMS added polymeric nanocomposite material would be synthesized in one step. Resol/clay nanocomposite resins were partially cured by heating. Spectroscopic, thermal, mechanical and microscopic properties of the final nanocomposite samples have been searched and determined by FTIR-ATR spectroscopy, differential scanning calorimetry (DSC), thermogravimetric analyzer (TGA), dynamic mechanical analyzer (DMA) and scanning electron microscopy (SEM).

EXPERIMENTAL

Materials

Phenol and formaldehyde solution (37%) were supplied by Riedel-de Haen and LAB-SCAN respectively for synthesis of resol resin. Sodium hydroxide pellets were supplied by Riedel-de Haen. The nanofiller, sodium-montmorillonite (MMT) (Nanofil 757) was used from Süd-Chemie (Switzerland). It is a highly purified natural sodium montmorillonite with cation-exchange capacity of 80 meq/100 g medium particle size as <10 μm, and bulk density of $\sim$2.6 g cm^{-3}. α,ω- dihydroxy poly(dimethylsiloxane) (DH.PDMS) was the product of Goldschmidt Chemical Corporation (Germany). Molecular weight of DH.PDMS was 2500 ± 250.

Analysis

FTIR spectra was measured using model recorded Perkin-Elmer Spectrum One FTIR (ATR sampling accessory) spectrophotometer.

Morphology of products was examined by scanning electron microscope, ESEM XL30 ESEM-FEG Philips and the samples for the SEM measurement are prepared by gold coating.

Dynamic Mechanical Analysis assays of DH.PDMS-LC-PFRs nanocomposite resin samples (DH.PDMS-LC-PFR1, DH.PDMS-LC-PFR2, DH.PDMS-LC-PFR3, DH.PDMS-LC-PFR4) were operated with DMA Q800 V7.5 Build 127 with a heating rate of 3°C/min to 400°C and with a forcing rate of 2 N/min to18 N.

DSC thermograms were obtained by using Perkin-Elmer DSC-6 instrument (USA); the heating rate was 10°C/min under a nitrogen atmosphere.

TGA was carried out in nitrogen atmosphere at a heating rate 10°C/min up to 900°C temperature by Perkin-Elmer Pyris 1. Weight loss (%) of samples was calculated at temperature range 20–900°C.

Preparation of Phenol Formaldehyde Resin (PFR)

Into a three-necked flask equipped with a stirrer, 9,4 g (0,1 mol) of phenol and 16.5 mL (0,2 mol) of formaldehyde solution (37%) were added. The temperature was raised to 65–70°C to start reflux. After raising the pH to 10 by addition of a 20% aqueous NaOH solution, the reaction mixture was kept in water bath for 4 h. After the 4-h periods, colorless sample solution became brownish and it was transferred in a two-necked round bottomed flask, then mixture was stirred with a magnetic stirrer for more 4 h at 70°C. During the reaction, viscosity of the mixture increased and at the end of the reaction, a very viscous resin was obtained in the form of a gel. The obtained resin

was dried under vacuum for 3 h at 65°C. By the effect of heat a solid and reddish resin sample was obtained.

Modification of Phenol Formaldehyde Resin (PFR) with DH.PDMS(DH.PDMS-PFR)

Into a three-necked flask equipped with a stirrer, 9.4g (0.1 mol) of phenol, 16.5 mL (0.2 mol) of formaldehyde solution (37%) and 2 mL of DH.PDMS were added. The temperature was raised to 65–70°C to start reflux. After raising the pH to 10 by addition of a 20% aqueous NaOH solution, the reaction mixture was kept in water bath for 4 h. After 4 ho, colorless sample solution became brownish and it was transferred in a two-necked round bottomed flask, then mixture was stirred with a magnetic stirrer for more 4 h at 70°C. During the reaction, viscosity of the mixture increased and at the end of the reaction, a very viscous resin was obtained in the form of a gel. The obtained resin was dried under vacuum for 3 h at 65°C. By the effect of heat a solid and reddish resin sample was obtained.

Preparation of DH.PDMS Modified Resol/Clay Nanocomposite Resins (DH.PDMS-LC-PFR)

DH.PDMS-LC-PFR was synthesized in four different initial pristine clay feed contents by weight (0.5, 1, 3, and 5 wt %). Constant ratio of monomers was 1 : 2 and constant amount of DH.PDMS of 2 wt % was applied at each polymerization. Unmodified montmorillonite clay was used to prepare resol/clay nanocomposite resins and the amount of the clays were 0.047 g for 0.5 wt % sample, were 0.094 g for 1 wt % sample, were 0.282 g for 3 wt % sample and were 0.47 g for 5 wt % sample. DH.PDMS-LC-PFR nanocomposite samples (DH.PDMS-LC-PFR1, DH.PDMS-LC-PFR2, DH.PDMS-LC-PFR3, DH.PDMS-LC-PFR4) were synthesized by the same way and by the same experimental setup with DH.PDMS-PFR. Contents of nanocomposite resins were summarized in Table I.

Preparation of Thin Films from PFR, DH.PDMS-PFR and DH.PDMS-LC-PFR

The same procedure was applied to synthesize film samples; mixtures were stirred until a viscous solution was obtained and schematically drawn in Figure 1. The solvent(dichloromethane) casting of the viscous solution was performed as film on 5 × 5 cm^2 glass substrate area at about 1 mm height. Homogeneous viscous film was dried under vacuum at 70°C. Afterward vacuum film samples were dried at 100°C in a drying oven for 1 h.

RESULTS AND DISCUSSION

Preparation of *in situ* modified phenol formaldehyde resin with DH.PDMS, clay were studied in the presence of base catalyst. Under alkaline conditions, the initial reaction product of phenol and formaldehyde is a mixture of *ortho*- and *para*-methylolated phenols. The methylolated phenols are more reactive with formaldehyde than the unsubstituted phenol, resulting in the rapid formation of 2, 4-dimethylolphenol and subsequently, 2, 4, 6-trimethylolphenol; the latter is the predominant product, with a large excess of formaldehyde and relatively short reaction time. DH.PDMS probably combines with the resin molecules from its hydroxy chain ends by the effect of base-catalyzed condensation reactions. Polymerization occurs primarily by a methylol group connected to a phenol group reacting at the ortho or para position of another phenol group to form a methylene bridge, connecting the two phenols. Dibenzylether bridges connecting two phenols are also formed by the reaction of two methylol groups with each other. With excess formaldehyde, methylol groups are present on the terminal phenol groups of resole resins. We prepared DH.PDMS modified PF resin and four DH.PDMS-LC-PFRs by one step. Formation of DH.PDMS-LC-PFR is shown in Scheme 1.

Table I. Contents of Resin Samples

Sample name	Clay content (wt %)	Molar ratio of P : F	DH.PDMS (wt %)
PFR	0	1 : 2	0
DH.PDMS-PFR	0	1 : 2	2
DH.PDMS-LC-PFR1	0,5	1 : 2	2
DH.PDMS-LC-PFR2	1	1 : 2	2
DH.PDMS-LC-PFR3	3	1 : 2	2
DH.PDMS-LC-PFR4	5	1 : 2	2

To characterize the chemical structure of PFR, DH.PDMS-PFR) DH.PDMS-LC-PFR1, DH. PDMS-LC-PFR2, PDMS-LC-PFR3, PDMS-LC-PFR4, the samples were subjected to FTIR analyses. The spectra were presented in Figures 2–4 and prominent peaks are identified. The FTIR spectrum of the PFR was given in Figure 2, and was recorded in the absorbance mode. The spectrum of uncured resol sample was recorded in the solid state without KBR. The characteristic peaks of PFR were observed at 3271 cm^{-1}, 1595 cm^{-1}, 1456 cm^{-1}, and 1117 cm^{-1} corresponding to –OH groups, C=C aromatic ring vibrations, methylene bridge —C—H and methylene ether bridge —C—O—C— band, respectively. *In situ* modification of PFR was achieved with DH.PDMS. As shown in Figure 3; in addition to the characteristic peaks of PFR, Si—O—Si stretching peak of DH.PDMS was also obtained for DH.PDMS-PFR at 1020 cm^{-1}. Uncured modified resol resins and cured resins, a reference band of 1595 cm^{-1} was used. This corresponds to stretching of the aromatic ethylene bond (—C=C—) in the aromatic ring which seems to be

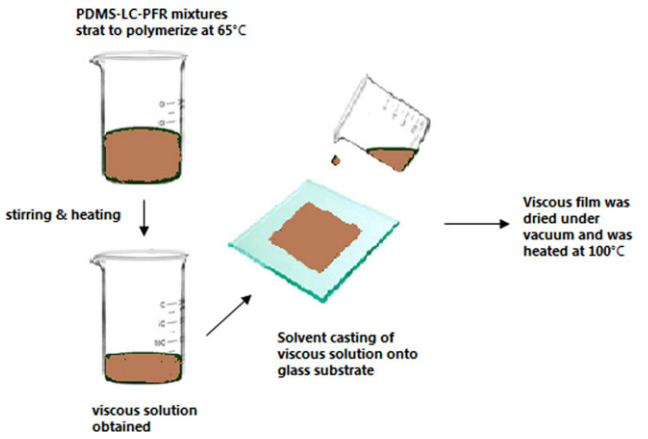

Figure 1. Preparation of thin films. [Color figure can be viewed in the online issue, which is available at wileyonlinelibrary.com.]

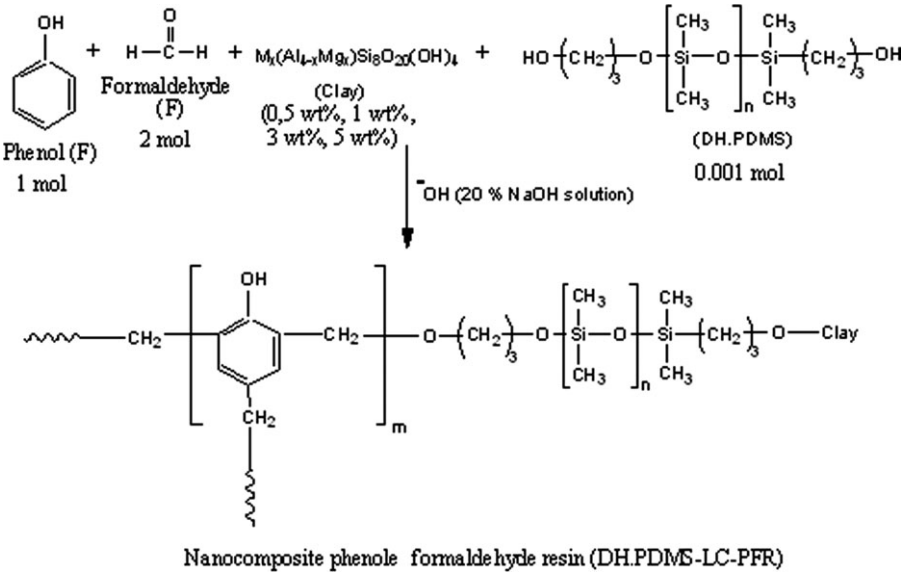

Scheme 1. Formation of Nanocomposite phenol formaldehyde resin (DH.PDMS-LC-PFR).

invariant. The out of plane C—H deformation in the monosubstituted benzene ring, and appears at 690 cm^{-1}. The at around 756 cm^{-1} corresponds to a 1,2-disubstituted benzene ring, and a 1,2,6-trisubstituted benzene ring. The peak at 826 cm^{-1} is attributable ton 1,4 and 1,2,4-substitution, and the 888 cm^{-1} peak was identified as a 1,2,4,6-tetrasubstituted benzene ring. The addition reactions on the free para-position occur in almost the same proportion as in each ortho-position of the phenol ring. Figure 4 shows the results for nanocomposite resins with different clay content. DH.PDMS-modified layered clay resol type phenol formaldehyde nanocomposite resins (DH.PDMS-LC-PFR1, DH.PDMS-LC-PFR2, DH.PDMS-LC-PFR3, DH.PDMS-LC-PFR4); were obtained through adding various amounts of unmodified montmorillonite clay, by *in situ* preparation method. Absorbances were obtained at about 2950 cm^{-1}, belonging to aliphatic C—H stretching bonds of resol (methylene bridge) in the FTIR spectra of nanocomposite resin. FTIR spectra of the nanocomposite resin samples were outlined in Figure 4 and the observed characteristic peaks of the PFR, DH.PDMS-CL-PFR1, DH.PDMS-CL-PFR2, DH.PDMS-CL-PFR3, and DH.PDMS-CL-PFR4 resin samples were demonstrated. As shown in Figure 4 by presence of DH.PDMS characteristic Si—O—Si bond peaks of samples were obtained excluding PFR and by adding clay, characteristic C—H stretching peaks of clay were observed for clay containing nanocomposite resin samples (PDMS-LC-PFR1, PDMS-LC-PFR2, PDMS-LC-PFR3, PDMS-LC-PFR4). Therefore, FTIR spectra of resin samples revealed that DH.PDMS and clay had effectively participated in polymerizations. As demonstrated in Figure 4, C—H stretching peaks of resol were slightly increased following increasing clay

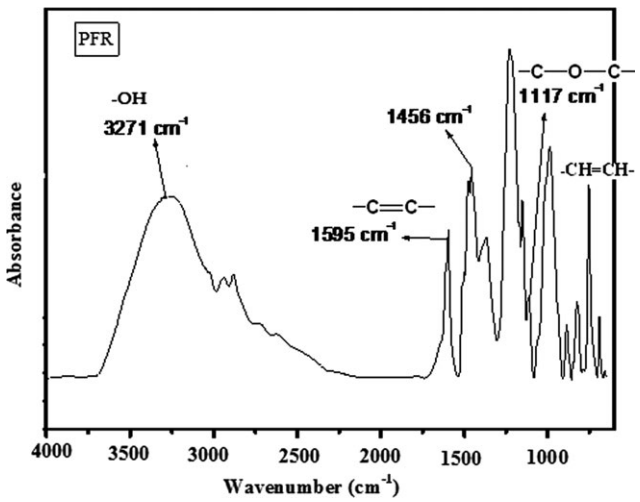

Figure 2. FTIR spectrum of PFR.

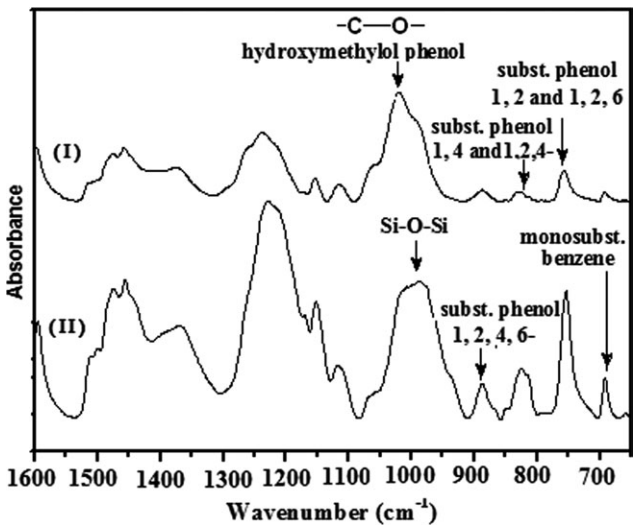

Figure 3. FTIR spectra of (I) phenol formaldehyde resin (PFR), (II) DH.PDMS modified phenol formaldehyde resin (DH.PDMS-PFR).

Applied Polymer SCIENCE

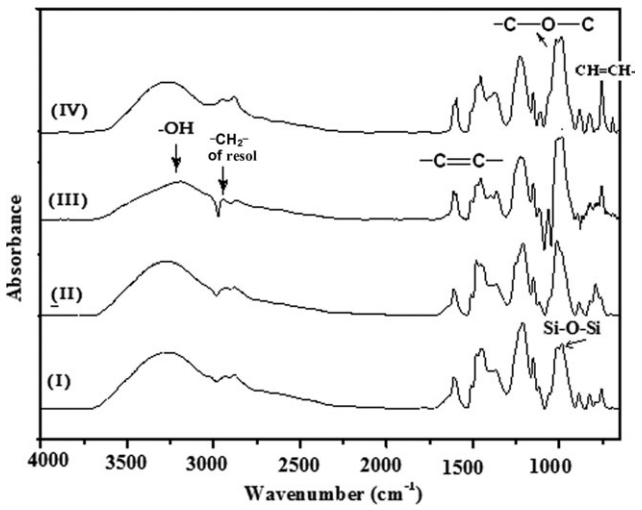

Figure 4. FTIR spectra of nanocomposite resin samples (I) DH.PDMS-CL-PFR1, (II) DH.PDMS-CL-PFR2, (III) DH.PDMS-CL-PFR3, (IV) DH.PDMS-CL-PFR4.

content up to 3 wt %, then they were decreased for the sample with 5 wt % clay content. Also the —OH content in plain peaks of samples was increased with increasing clay content from 0.5 to 5 wt %. A maximum quantity of disubstituted (1,2 and 1,2,6) phenol was found for the DH.PDMS-CL-PFR4 (line 4 in Figure 4). However, the quantity of the mono substituted phenol compounds disappear with the DH.PDMS-CL-PFR1, DH.PDMS-CL-PFR2, DH.PDMS-CL-PFR3 (line 1, 2, and 3 in Figure 4), as a consequence of the higher degree of conversion.

Thermal behavior of resins was examined by differential scanning calorimetry (DSC) in the range of 20–170°C and by thermogravimetric analysis (TGA) in the range of 20–900°C. Differential Scanning Calorimeter (DSC) measurements of PFR, DH.PDMS-LC-PFR1, DH.PDMS-LC-PFR2, DH.PDMS-LC-PFR3, and DH.PDMS-LC-PFR4 were performed for 1 cycle. The cycle was heated from 30 to 160°C with 10°C/min heating rate. Thermal behavior of DH.PDMS-PFR was examined by differential scanning calorimetry in the range of 20 to 170°C

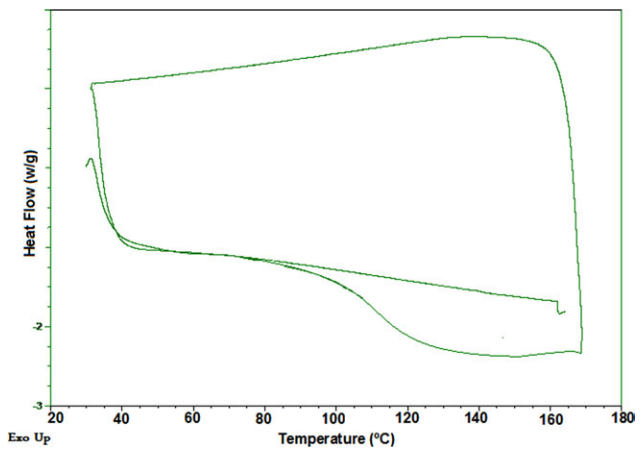

Figure 5. DSC thermograms for DH.PDMS-PFR. [Color figure can be viewed in the online issue, which is available at wileyonlinelibrary.com.]

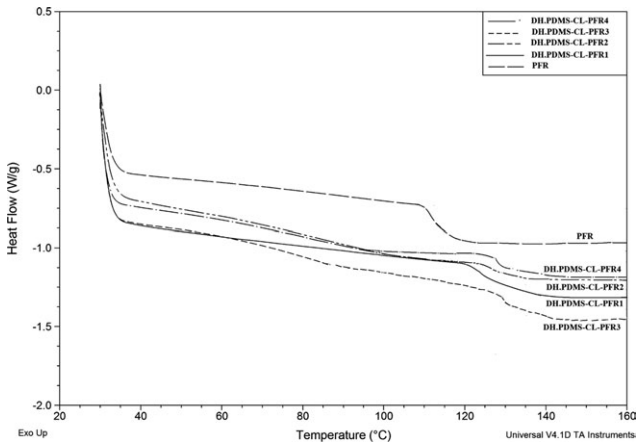

Figure 6. DSC thermograms for PFR, DH.PDMS-LC-PFR1, DH.PDMS-LC-PFR2, DH.PDMS-LC-PFR3, and DH.PDMS-LC-PFR4 samples.

(Figure 5) for 3 cycle. The T_g value of DH.PDMS-PFR is about 116°C. DSC measurement on DH.PDMS-PFR with over again exhibited no glass transition, indicating that the heated to 170°C resin is crosslink. In this study T_g values of the PFR, DH.PDMS-LC-PFR1, DH.PDMS-LC-PFR2, DH.PDMS-LC-PFR3, and DH.PDMS-LC-PFR4 were determined as 109, 122, 124, 128, and 123°C, respectively. As shown in the Figure 6, it was observed from the results of DSC measurements that, T_g values of the DH.PDMS-PFR and DH.PDMS-LC-PFRs are higher than PFR. Also T_g values of clay containing samples slightly change with the increasing clay content (wt %), so that they increase up to 3 wt % clay contents and then they decrease for the sample with the 5 wt % clay content (Figure 7).

Resin samples were partially cured by heating at 100°C for a 1 h. The curing reaction involves condensation reactions of hydroxymethyl groups that were previously formed through reaction of phenol with excess formaldehyde in the presence of an alkaline catalyst in order to form methylene bridges of the

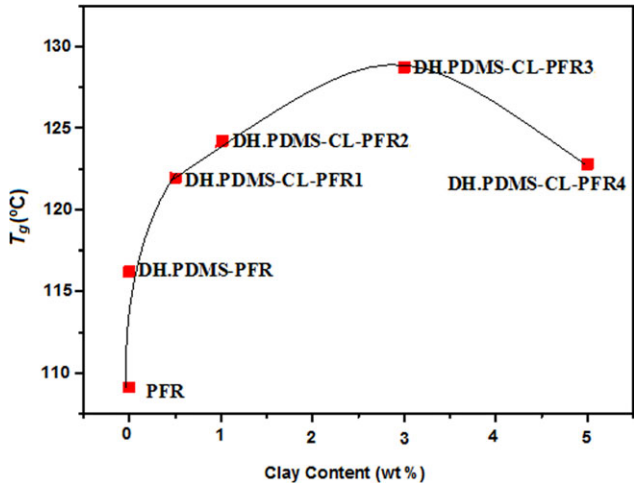

Figure 7. Variation of T_g (°C) for various resole clay reinforced nanocomposites with different filler content. [Color figure can be viewed in the online issue, which is available at wileyonlinelibrary.com.]

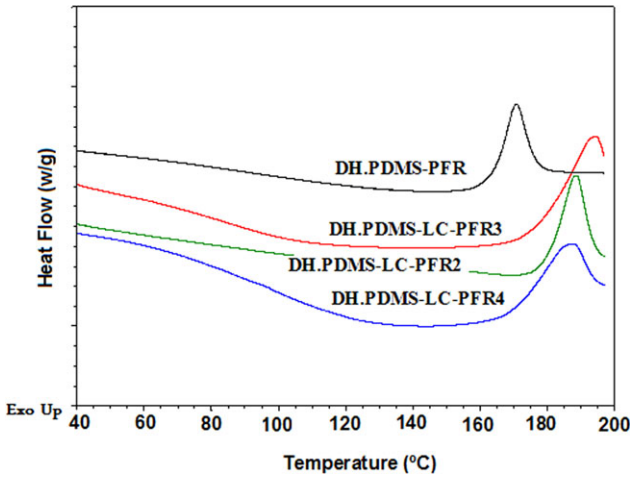

Figure 8. DSC thermograms for cured DH.PDMS-PFR, DH.PDMS-LC-PFR2, DH.PDMS-LC-PFR3, and DH.PDMS-LC-PFR4 samples. [Color figure can be viewed in the online issue, which is available at wileyonlinelibrary.com.]

resols. As shown in Figure 8, the shape and the maximum of the exothermic curves depended on the given curing temperature and time. In order to remove H_2O and volatile components, the uncured resin required a heat-treatment at 100°C for 60 min prior to curing or molding. As demonstrated in Figure 8, and observed from the results of DSC measurements exothermic peaks were observed in between 165 and 195°C for the curing reactions in this study.

The aim of DSC measurement for cured phenolic resins is the determination of maximum cure temperatures and onset of curing temperatures. Maximum curing temperatures and onset of curing temperatures of PFR, DH.PDMS-PFR (Figure 9), DH.PDMS-LC-PFR2, DH.PDMS-LC-PFR3, and DH.PDMS-LC-PFR4 were determined consistently with the literature values.[30] According to Harper,[31] maximum curing temperature or upper use temperature of the adhesive may dictate the maximum temperature of environmental exposure belonging to the compo-

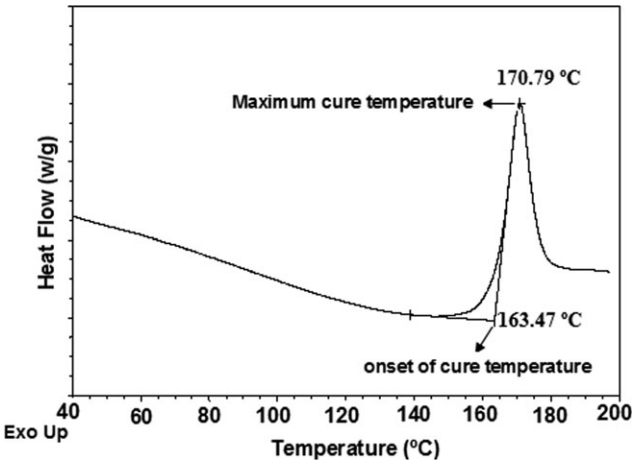

Figure 9. Determination of the maximum cure temperature and onset of cure temperature for cured DH.PDMS-PFR from DSC plot.

Table II. Maximum Cure Temperature and Onset of Cure Temperature Values for Samples

Sample	Maximum cure temperature (°C)	Onset of cure temperature (°C)
PFR	168.42	167.02
DH.PDMS-PFR	170.79	163.47
DH.PDMS-LC-PFR2	188.68	185.64
DH.PDMS-LC-PFR3	194.65	176.18
DH.PDMS-LC-PFR4	187.62	186.05

nent. There are several curing temperature ranges. As shown in Table II and Figure 9, clay containing resin samples DH.PDMS-LC-PFR2, DH.PDMS-LC-PFR3, and DH.PDMS-LC-PFR4 have maximum curing temperatures above 176°C and could be used for aircraft applications.

Manfredi et al.[23] and Roczniak et al.[32] identified the region between 1500 and 1400 cm^{-1} as characteristic for the deformation vibration of —CH— bonds in —CH_2— groups and some differences can be noticed. These differences can yield information as to the structure of methylene bridge. Figure 10 shows the FTIR spectra for different DH.PDMS-LC-PFRs after the crosslinking reaction. The band at ~1450 cm^{-1} was assigned to methylene bridge in p-p', the band at 1460 cm^{-1} was assigned

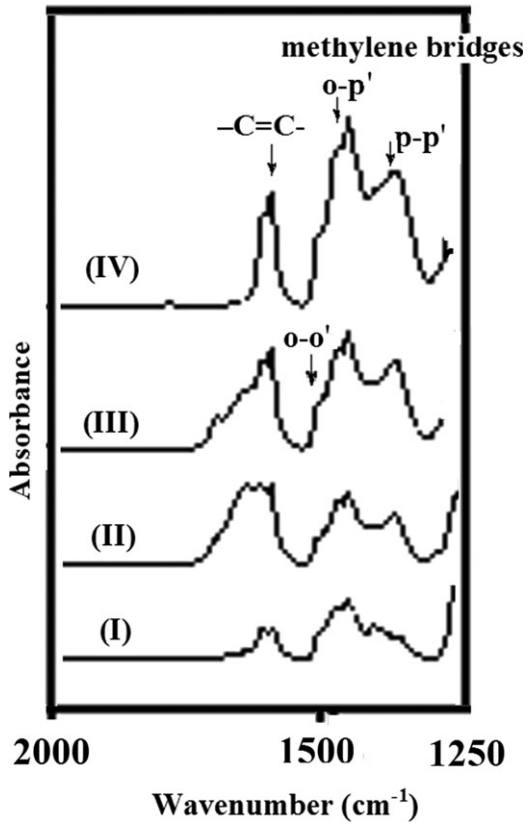

Figure 10. FTIR spectra of the fully cured nanocomposite resins; (I) DH.PDMS-CL-PFR4, (II) DH.PDMS-CL-PFR1, (III) DH.PDMS-CL-PFR2, (IV) DH.PDMS-CL-PFR3.

Applied Polymer SCIENCE

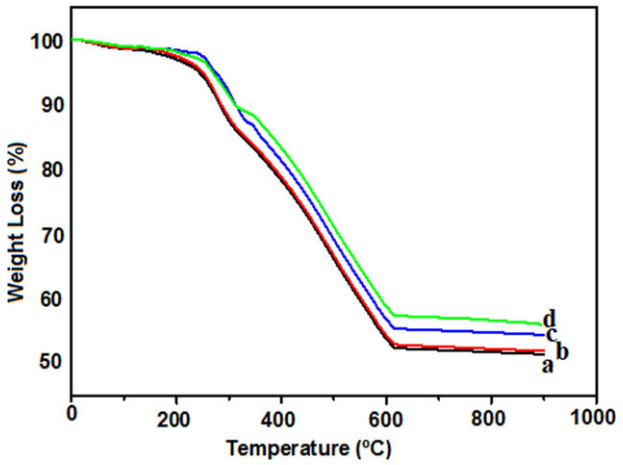

Figure 11. TGA thermograms of (a) PFR, (b) DH.PDMS-LC-PFR1, (c) DH.PDMS-LC-PFR3, (d) DH.PDMS-LC-PFR4. [Color figure can be viewed in the online issue, which is available at wileyonlinelibrary.com.]

to the methylene bridge in o-o' and the band at 1480 cm^{-1} was assigned to the o-p' position. These bands are higher for completely cured resols than for the prepolymer or uncured resols. It is an indication that more crosslinking reaction occurs in the curing step than during the synthesis of the resols. The applications of this analysis to the resols allows us to determine that the quantity of p-p' bridge is higher than that of the o-p' bridge, and that the o-o' bridge was not found in the resol. A higher proportion of methylene bridge found for the clay content of nanocomposite resins between 0.5 and 3.

Thermal decomposition behavior of neat resol; PFR and clay-filled nanocomposite resins; DH.PDMS-LC-PFR1, DH.PDMS-LC-PFR3, and DH.PDMS-LC-PFR4 were determined via TGA measurements. In order to prepare TGA samples, resol resin and the clay-filled nanocomposite resol resins were partially cured at 100°C for 1 h. A powder sample of 5 mg of the cured resin was subjected to TGA analysis, and heated at linear heating rate of 10°C. Degradation was carried out in a static air atmosphere until the maximum temperature of 900°C. The weight loss (wt %) of the resins was calculated; and the weight loss (%) rates are shown as a function of temperature in Figure 11 and Table III. López et al.,[33] different stages of degradation could be obtained in the TGA thermogram: the first stage (up to 350°C) and the second stage (350–700°C). In the first stage, formaldehyde release caused by breaking of ether bridges, and the presence of phenol and water, and in the second stage the oxidation of the network was observed. In this study, the first stage continued up to 300°C and second stage was observed in the temperature range 300–900°C. In the second stage of thermal decomposition, all the clay containing nanocomposite resins displayed higher thermal resistance than PFR. As shown in Figure 11 and Table III, the weight loss rates of common resol resins were higher than that of DH.PDMS-LC-PFR. Also, weight loss (%) rates of the clay-filled nanocomposite resins were decreased with increasing clay content. DH.PDMS-LC-PFR3 and DH.PDMS-LC-PFR4 seemed slightly more stable on thermal grounds because their thermal degradations started at higher temperatures than PFR and DH.PDMS-LC-PFR1.

Table III. TGA Results for Resins

Sample	Residue at 500°C (wt %)[a]	Residue at 900°C (wt %)[a]
PFR	66	51
DH.PDMS-LC-PFR1	67	52
DH.PDMS-LC-PFR3	70	54
DH.PDMS-LC-PFR4	72	56

[a]Detected by TGA.

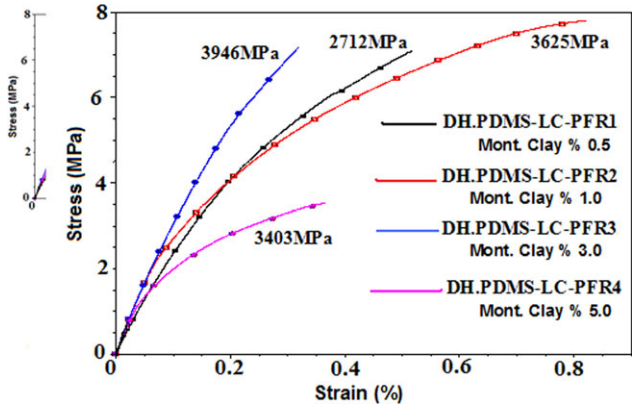

Figure 12. Stress–strain graphs of the DH.PDMS modified layered clay resole type phenol formaldehyde nanocomposite resin specimens. [Color figure can be viewed in the online issue, which is available at wileyonlinelibrary.com.]

The final properties of the nanocomposite resins were determined using dynamical mechanical tests. DMA Q800 V7.5 Build 127 units was used with a fixed frequency at 1 Hz and a heating rate of 3°C/min in a three-point bending mode. The specimen bars used for these tests were cut from plaques obtained by curing the nanocomposite resin between two thin glasses previously treated with the silicone release agent from Siliar S.A. Argentina. Dynamic mechanical analysis of cured resol was performed in Figure 12.

Young's Modulus Measurements

Young's modulus values of the DH.PDMS-LC-PFR1, DH.PDMS-LC-PFR2, DH.PDMS-LC-PFR3, and DH.PDMS-LC-PFR4 thin film specimens were obtained from stress–strain curves of DMA measurements. The slope of the stress–strain curve gives the Young's modulus of the sample. As it is seen from Figure 12; slopes of the stress-strain curves are considerably steep, that means in order to deform the samples much force is needed. Therefore, Young's modulus values of the samples were relatively high, which were detected as 2712 MPa for DH.PDMS-LC-PFR1, 3625 MPa for DH.PDMS-LC-PFR2, 3946 MPa for DH.PDMS-LC-PFR3, and 3403 MPa for DH.PDMS-LC-PFR4. Elasticity properties of the samples were generally similar, but DH.PDMS-LC-PFR2 had a higher elongation than DH.PDMS-LC-PFR1, DH.PDMS-LC-PFR3, and DH.PDMS-LC-PFR4.

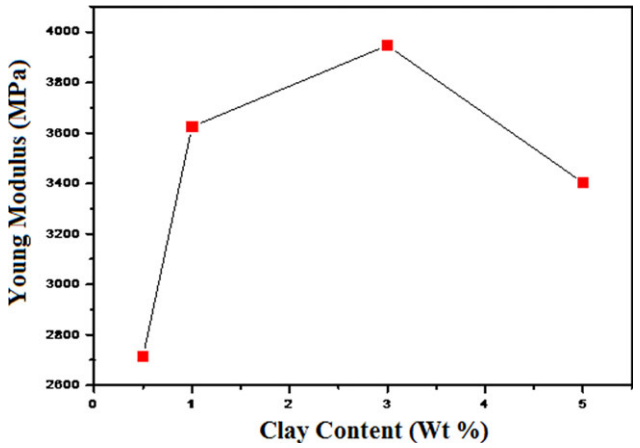

Figure 13. Variation of Young's modulus (MPa) for various layered clay resole nanocomposites with different filler content. [Color figure can be viewed in the online issue, which is available at wileyonlinelibrary.com.]

The specimen with the highest clay content (5%) have lower crosslink density than other specimens with lower clay content (0.5, 1, and 3%). Since increasing the clay content led to worse dispersion of clay particles in the polymer matrix, crosslinking of polymers may be hindered due to decreased movability between chains. Decreasing the crosslink density resulted in a decrease in the Young's modulus value of the sample. As it is seen in Figure 13, Young's modulus values of the samples were slightly increased with increasing clay content until 3%, then it was decreased for the sample with 5% clay content (DH.PDMS-LC-PFR4), since it had the clay content above optimum values. DH.PDMS-LC-PFR3 sample had the highest Young's modulus value among the samples.

Thermal Measurements

Glass transition temperature values of the DH.PDMS-LC-PFR1, DH.PDMS-LC-PFR2, DH.PDMS-LC-PFR3, and DH.PDMS-LC-PFR4 thin film samples were determined according to three different parameters (storage modulus, loss modulus, tan delta) by dynamic mechanical analysis method. Parameter that gave the nearest results for T_g values of the specimens was tan delta in DMA measurements. DH.PDMS-LC-PFR3 sample had the highest T_g value among all samples. As it is seen in Table IV, this result is in agreement with T_g results observed from DSC measurements of the specimens. According to the DMA measurements, DH.PDMS-LC-PFR3 (3 wt % clay containing sample) has better thermal and mechanical properties than other resins.

Table IV. Observed T_g Values of Samples from DMA and DSC Measurements

	T_g (°C)			
Sample	Storage modulus (E')	Loss modulus	Tan delta (δ)	DSC
DH.PDMS-LC-PFR1	50.63	90.10	104	122
DH.PDMS-LC-PFR2	53.54	92.63	105.95	124
DH.PDMS-LC-PFR3	57.86	94.80	130.37	128
DH.PDMS-LC-PFR4	55.65	107.46	125.61	123

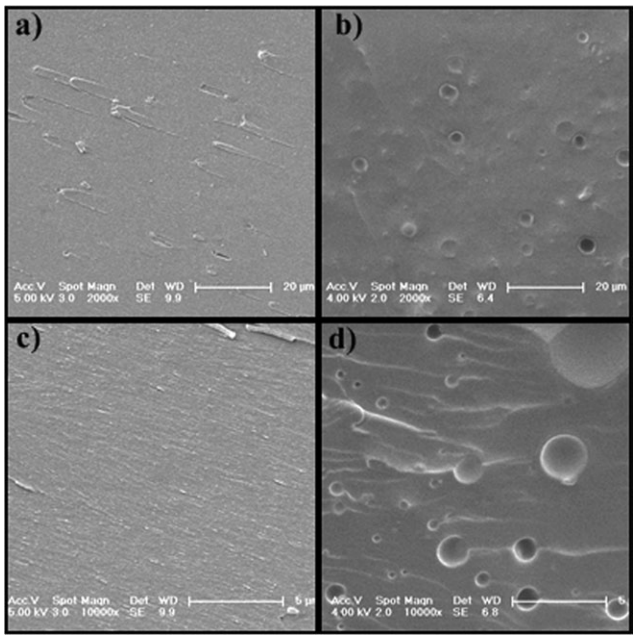

Figure 14. SEM images of (a) PFR, (b) DH.PDMS-PFR, (c) PFR, (d) DH.PDMS-PFR.

Scanning Electron Microscope Measurements (SEM)

SEM analysis was performed to understand the distribution of clay particles in polymeric resol resin matrix and in order to gain an idea about the degree of intercalation and/or exfoliation of the clay layers. SEM images of the PFR, DH.PDMS-PFR, DH.PDMS-CL-PFR1, DH.PDMS-CL-PFR2, DH.PDMS-CL-PFR3, and DH.PDMS-CL-PFR4 were taken from their thin film samples. SEM images of PFR and DH.PDMS-PFR are shown in Figure 14 with 2000× and 10000× magnification. As seen in Figure 14 the formation of micro and macrovoids were observed in SEM images of DH.PDMS-PFR, due to release of by-product water molecules during the polymerization reaction of DH.PDMS-PFR, and the water vapor bubbles got trapped in the DH.PDMS-PFR during heat curing. Unlike PFR, adequately long the reaction time and waiting under vacuum conditions prior heat curing in the oven, was not enough to solve this problem for DH.PDMS-PFR. Tendency of DH.PDMS molecules to move towards the surface due to the difference in surface tension that induced voids formation is the reason why SEM images of DH.PDMS-PFR was not as clear as SEM images of the PFR.

SEM images of DH.PDMS-LC-PFR samples with magnification of 5000× are shown in Figure 15(a,b), PDMS-LC-PFR1 and DH.PDMS-LC-PFR2, were indicated and in c and d, with magnification of 10000× for DH.PDMS-LC-PFR3 and DH.PDMS-LC-PFR4, respectively. Good dispersion of clay particles was not problematic for samples with clay contents of 0.5, 1, and 3 wt %. But as it is seen in Figure 15, for DH.PDMS modified resole type phenolic resin with clay content of 5 wt % (DH.PDMS-LC-PFR4), clay particles were dispersed less homogeneously than

Applied Polymer SCIENCE

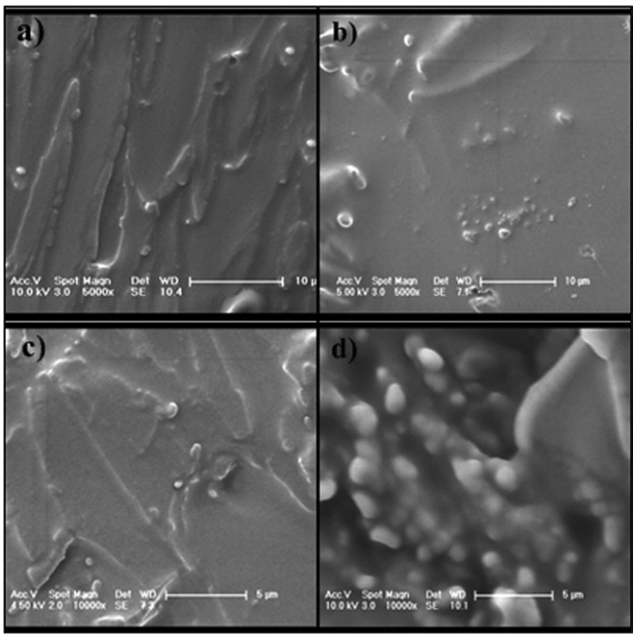

Figure 15. SEM images of (a) DH.PDMS-LC-PFR1, (b) DH.PDMS-LC-PFR2, (c) DH.PDMS-LC-PFR3, (d) DH.PDMS-LC-PFR4.

DH.PDMS-LC-PFR1, DH.PDMS-LC-PFR2, and DH.PDMS-LC-PFR3.

High surface energy of nanoparticles forced them to agglomerate and to form clay tactoids. Therefore, resol type phenolic resins with clay content higher than 1.5% had problems in the homogeneous dispersion of clay particles. Dispersion can be improved by using techniques like high shear mixing and ultrasonification. DH.PDMS was added in the media in order to improve the surface properties of the material and to decrease the surface energy of the nanoparticles. As a result, the resins with clay contents of 3, 1, and 0.5 wt % had good dispersion of clay particles, and had good material properties. Higher amount of clays required higher rates of mixing in order to intercalate the polymer into the clay layers and homogeneously distribute these layers in the polymer matrix. However, bubbles trapped and the spaces formed in the resin sample increased with higher mixing rates, and formation of the material weakening clay tactoids resulted in worsening of mechanical properties of the DH.PDMS-LC-PFR4 resin.

Effect of the Reaction Time

DH.PDMS-LC-PFR4 were synthesized in four different reaction times (2, 4, 6, and 8 h). FTIR analysis was performed for all reaction times and spectrums were compared in order to examine the effect of the reaction time on the polymerization of the nanocomposite resins. As seen in Figure 16, characteristic absorbance peaks of DH.PDMS-LC-PFR4 exhibited differences to be specific to the various reaction times. According to the FTIR spectrum for the 2-h reaction (see Figure 16 (line 1) characteristic —OH groups, aromatic ring C=C bond and methylene bridge peaks were decreased since the polymerization was not completed. Also C—H stretching peak of resol and C—H out-of-plane peaks of the sample with 2-h reaction time are more

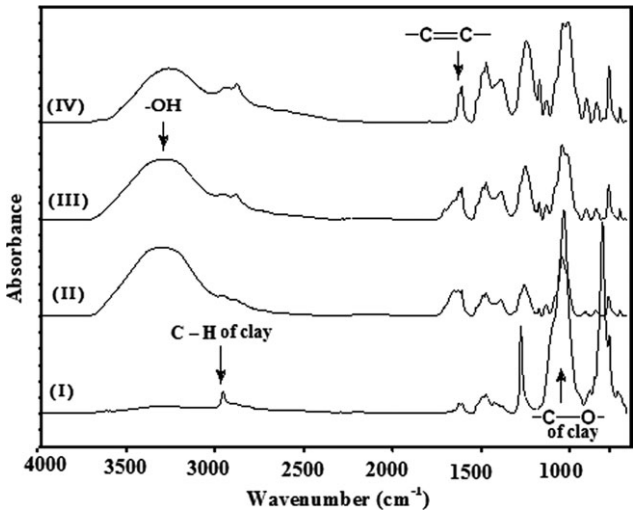

Figure 16. FTIR spectra of the resins with the clay content 5% (DH.PDMS-LC- PFR4) and with the different reaction times; (I) 2 h, (II) 4 h, (III) 6 h, (IV) 8 h.

intensive and sharper than the peaks of other samples with higher reaction times. With increasing reaction time from 4 to 8 h, absorbance intensity of the —OH groups peaks decreased. The intensity of the —OH peaks for the 4-h reaction is higher than that for 6 and 8 h reactions due to coexistence of the methylol —OH peaks with phenolic —OH peaks in 4-h reaction. Methylol groups were formed at the beginning of the polymerization by the reaction of the phenol and formaldehyde. With increasing reaction time, the amount of branching of DH.PDMS-LC-PFR4 increased and of methylol groups decreased due to formation of the methylene bridges instead of

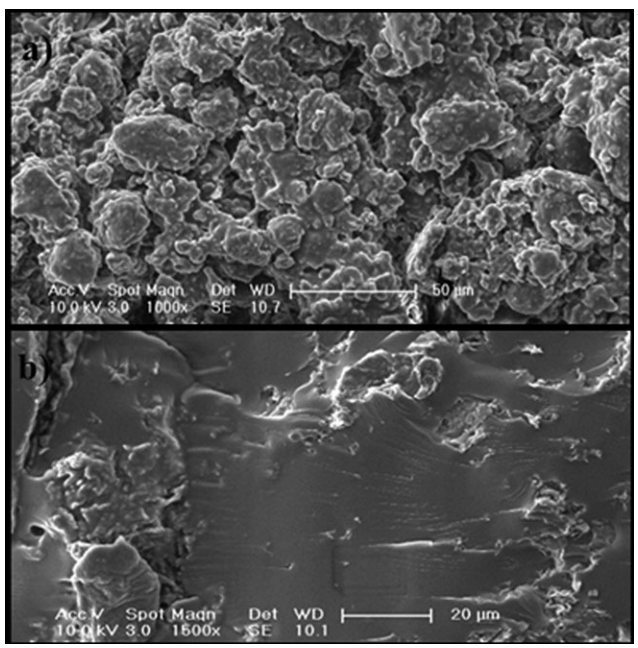

Figure 17. SEM images of the DH.PDMS-LC-PFR4 for (a) 2 h and (b) 8 h reaction time.

methylol groups. Therefore, with increasing reaction time, characteristic methylene bridge peaks of DH.PDMS-CL-PFR4 increased. Also as shown in Figure 16, as the reaction continued, the aromatic H—C=C—H peaks decreased and C—O—C methylene ether bridge peaks increased. Because, polymerization occurs primarily by a methylol group connected to a phenol group reacting at the ortho or para position of another phenol group to form a methylene bridge, connecting the two phenols. Dibenzylether bridges connecting two phenols are also formed by the reaction of two methylol groups with each other or unsubstituted phenol.

As seen in Figure 17, SEM images of the same sample with different reaction times exhibited noticeable differences. SEM image of 2-h reaction looked like clay particles rather than a nanocomposite resin. For 2-h reaction, sizes of clay tactoids were larger and dispersion of the clays were worse than for 8-h reaction. As explained earlier in the SEM analysis section, 5 wt % clay content is above the limit in this study and high clay content is needed to increase the mixing rate and to extend the reaction time. Therefore, 2 h were not enough to complete the polymerization.

CONCLUSIONS

In this study, DH.PDMS *in situ* modified layered clay resol nanocomposites resins were synthesized. DSC analysis showed that the T_g and maximum curing temperature values of neat resol resin was increased by adding DH.PDMS and clay to obtain nanocomposite resins. T_g values of uncured nanocomposite resins and maximum curing temperatures of cured nanocomposite resins were slightly increasing by increasing clay content up to 3 wt %, then decreased for the sample with 5 wt % clay content. Furthermore, DH.PDMS-LC-PFR2, DH.PDMS-LC-PFR3, and DH.PDMS-LC-PFR4 nanocomposite resins had maximum curing temperatures above 176.67°C and could be used for aircraft applications. The increasing clay content induced the decrease in weight loss (wt %) rates of nanocomposite resins. DMA analysis demonstrated that DH.PDMS-LC-PFR3 had the highest Young's modulus value and elasticity properties of the samples were generally similar, but DH.PDMS-LC-PFR2 had higher elongation than other nanocomposite resins. Also, T_g values of resins determined by DMA were supported by DSC results. DH.PDMS was added in the media to improve the surface properties of the material and in order to decrease the surface energy of the nanoparticles. Thus, SEM measurements showed that the nanocomposite resins with the clay content of 3, 1, and 0.5 wt % had a good dispersion of clay particles, and had good material properties. However, in the DH.PDMS-LC-PFR4, clay particles were dispersed less homogeneously than DH.PDMS-LC-PFR1, DH.PDMS-LC-PFR2, and DH.PDMS-LC-PFR3. Finally, effect of the reaction time was investigated. The 2-h reaction time of clay tactoids are much and dispersion of the clays was worse than for 8-h reaction. The synthesis structure and thermal, and mechanical properties of DH.PDMS *in situ*-modified layered clay resol nanocomposite resins have not been investigated until now. In conclusion, clay particles were successfully dispersed in resol resin matrix and nanocomposites resins with better thermal and mechanical properties were obtained which can be used for thermal insulation materials, coatings, molding compounds, and aerospace components.

ACKNOWLEDGMENTS

The authors thank the Istanbul Technical University Research Foundation (İTÜ-BAP Project No: 34389).

REFERENCES

1. Kizilcan, N.; Akar, A. *J. Appl. Polym. Sci.* **2005**, *98*, 97.
2. Usuki, A.; Kawasumi. M.; Kojima, Y. *J. Mater. Res.* **1993**, *8*, 1174.
3. Lee, S. M.; Hwang, T. R.; Lee, J. W. *Polym. Eng. Sci.* **2004**, *44*, 1170.
4. Chen, B.; Evans, J. R. G. *Polym. Int.* **2005**, *54*, 807.
5. Garcia-Lopez, D.; Gobernado-Mitre, I.; Fernandez, J. F.; Pastor, J. M. *Polymer* **2005**, *46*, 2758.
6. Tortora, M.; Gorrasi, G.; Vittoria, V.; Chiellini, E. *Polym. J.* **2002**, *43*, 6147.
7. Becker, O.; Varley, R.; Simon, G.; *Polymer* **2002**, *43*, 4365.
8. Liu, T. X.; Liu, Z. H.; Ma, K. X.; He, C. B. *Compos. Sci. Technol.* **2003**, *63*, 331.
9. McNally, T.; Murphy, W. R.; Lew, C. Y.; Brennan, G. P. *Polymer* **2003**, *44*, 2761.
10. Ray, S. S.; Okamoto; M. *Prog. Polym. Sci.* **2003**, *28*, 1539.
11. Dubois, P.; Alexandre, M. *Mater. Sci. Eng.* **2000**, *28*, 1.
12. Zhi, L.; Zhao, T.; Yu, Y. *Scripta Materialia* **2002**, *47*, 875.
13. Choi, M. H.; Chung, I. J.; Lee, J. D. *Chem. Mater.* **2000**, *12*, 2977.
14. Byun, H. Y.; Choi, M. H.; Chung, I. J. *Chem Mater* **2001**, *13*, 4221.
15. Zhang, Z.; Ye, G.; Toghiani, H. *Macromol. Mater. Eng.* **2010**, *295*, 923.
16. Yilgor, E.; Eynur, T.; Kosak, C.; Bilgin, S.; Yilgor, I.; Malay, O.; Menceloglu, Y.; Wilkes, L. *Polymer* **2011**, *52*, 4189.
17. Brown, N.; Linnert, E.; Bühl, D. *Composites* **1996**, *14*, 29.
18. Gardziella, A.; Pilato, L. A.; Knop, A. Phenolic Resins, 2nd ed., Springer-Verlag: Berlin, **2000**, p 29.
19. Astarloa-Aierbe, G.; Echeverría, J. M.; Martín, M. D.; Etxeberria, A. M.; Mondragon, I. *Polymer* **2002**, *43*, 2239.
20. Astarloa-Aierbe, G.; Echeverri'a, J. M.; Marti'n, M. D.; Etxeberria, A. M.; Mondragon, I. *Polymer* **2000**, *41*, 3311.
21. Riccardi, C. C.; Astarloa-Aierbe, G.; Echeverrí'a, J. M.; Mondragon, I. *Polymer* **2002**, *43*, 1631.
22. Gabilondo, N. Ph.D. Thesis, Euskal Herriko Unibertsitatea/ Universidad del País Vasco, Donostia-San Sebastián, España, **2004**.
23. Manfredi, L. B.; Osa, de la O.; Fernandez, G. N.; Vazquez, A. *Polymer* **1999**, *40*, 3867.
24. Liu, W.; Hoa, S. V.; Pugh, M. *Compos. Sci. Technol.* **2005**, *65*, 307.

25. Byun, H. Y.; Choi, M. H.; Chung, I. J. *Chem. Mater.* **2001**, *13*, 4221.

26. Kaushik, A.; Singh, P.; Verma, G. *J. Therm. Plastic Comp. Mater.* **2010**, *23*, 79.

27. Manfredi, L. B.; Puglia, D.; Kenny, J. M.; Vazquez, A. *J. Appl. Polym. Sci.*, **2007**, *104*, 3082.

28. Kaynak, C.; Tasan, C. C. *Euro. Polym. J.* **2006**, *42*, 1908.

29. Lopez, M.; Blanco, M.; Vazquez, A.; Gabilondo, N.; Arbelaiz, A.; Echeverria, J. M.; Mondragon, I. *Thermochim. Acta* **2008**, *467*, 73.

30. Pilato, L. *Phenolic Resins*: A Century of Progress, 1st ed., Springer-Verlag: Berlin Heidelberg, **2010**, p 121.

31. Harper, C. A. Handbook of Plastics, Elastomers, and Composites. 4th ed., R. R. Donnelley & Sons Company **2010**, p 307.

32. Roczniak, C.; Biernacka, T.; Skarzynski M. *J. Appl. Polym. Sci.* **1983**, *28*, 531.

33. López, M.; Blanco, M.; Ramos, J. A.; Vazquez, A.; Gabilondo, N.; del Val, J. J.; Echeverri'a, J. M.; Mondragon, I. *J. Appl. Polym. Sci.* **2007**, *106*, 2800.